Phytochemistry 94 (2013) 198–205

Contents lists available at SciVerse ScienceDirect

Phytochemistry

journal homepage: www.elsevier.com/locate/phytochem

Thielavins A, J and K: α-Glucosidase inhibitors from MEXU 27095, an endophytic fungus from *Hintonia latiflora* ☆

José Rivera-Chávez [a], Martín González-Andrade [b], María del Carmen González [c], Anthony E. Glenn [d], Rachel Mata [a,*]

[a] Facultad de Química, Universidad Nacional Autónoma de México, México DF 04510, Mexico
[b] Instituto Nacional de Medicina Genómica (INMEGEN), Secretaría de Salud, Distrito Federal, C.P. 14610, México City, Mexico
[c] Instituto de Biología, Universidad Nacional Autónoma de México, México DF 04510, Mexico
[d] Toxicology & Mycotoxin Research Unit, 950 College Station Road, USDA ARS Russell Research Center, Athens, GA 30605, USA

ARTICLE INFO

Article history:
Received 21 March 2013
Received in revised form 16 May 2013
Available online 26 June 2013

Keywords:
Type II diabetes mellitus
Hintonia latiflora
Endophytic fungus
Thielavins
α-Glucosidase
Enzymatic inhibition
Molecular docking
Oral sucrose tolerance test

ABSTRACT

Bioassay-guided fractionation of the bio-active organic extract obtained from solid-media culture of MEXU 27095, an endophytic fungus isolated from the Mexican medicinal plant *Hintonia latiflora* (Rubiaceae), led to separation of three tridepsides which were identified as thielavins A, J and K. All three compounds inhibited *Saccharomyces cerevisieae* α-glucosidase (*αGHY*) in a concentration-dependent manner with IC_{50} values of 23.8, 15.8, and 22.1 μM, respectively. Their inhibitory action was higher than that of acarbose (IC_{50} = 545 μM), used as a positive control. Kinetic analysis established that the three compounds acted as non-competitive inhibitors with k_i values of 27.8, 66.2 and 55.4 μM, respectively (α = 1.0, 1.2, 0.7, respectively); acarbose behaved as competitive inhibitor with a k_i value of 156.1 μM. Thielavin J inhibited the activity of α-glucosidase from *Bacillus stearothermophilus* (*αGHBs*) with an IC_{50} of 30.5 μM, being less active than acarbose (IC_{50} = 0. 015 μM); in this case, compound (**2**) (k_i = 20.0 μM and α = 2.9) and acarbose (k_i = 0.008 μM and α = 1.9) behaved as non-competitive inhibitors. Docking analysis predicted that all three thielavins and acarbose bind to homologated *αGHBs* and to *αGHY* (PDB: 3A4A) in a pocket close to the catalytic site for maltose and isomaltose, respectively. The α-glucosidase inhibitory properties of thielavin K (**3**) were corroborated *in vivo* since it induced a noted antihyperglycemic action during an oral sucrose tolerance test (3.1, 10.0 and 31.6 mg/kg) in normal and nicotinamide–streptozotocin diabetic mice. In addition, at a dose of 10 mg/kg, it provoked a moderate hypoglycemic activity in diabetic mice.

1. Introduction

Diabetes mellitus is a polygenic complex metabolic disorder characterized by high blood glucose levels. This disease is one of the most challenging health problems to all nations in the 21st century. In 2010, an estimated 285 million people worldwide had diabetes mellitus, 90% of whom had type 2 diabetes mellitus (TII-DM) which is associated with low insulin production or insulin resistance due to genetic and/or epigenetic causes (Chen et al., 2011; Scully, 2012). Globally, the number of people with diabetes mellitus is projected to rise to 439 million by 2030. The serious complications associated with TII-DM, such as cardiovascular disease, peripheral vascular disease, stroke, diabetic neuropathy, amputations, renal failure, and blindness result in increasing disability, reduced life expectancy, and enormous health costs (Scully, 2012).

The best treatment for TII-DM involves hyperglycemic control using appropriate therapies and a healthy lifestyle. Most treatments focus on increasing insulin levels, improving sensitivity to the hormone in tissues, or reducing the rate of carbohydrate absorption from the gastrointestinal tract (Israili, 2011). The last group of drugs includes inhibitors of α-glucosidases, which catalyze the final step in the digestive process of carbohydrates and are useful to prevent the progression of the disease. α-Glucosidases are membrane-bound enzymes that hydrolyze the glycosidic bond of larger carbohydrate molecules to yield glucose and related monosaccharides. Therefore, α-glucosidase inhibitors delay glucose absorption and lower the postprandial blood glucose peak (Israili, 2011). The best known α-glucosidase inhibitors are acarbose, isolated from *Actinoplanes* species, and miglitol, an analogue of the natural product 1-deoxynojirimycin isolated from mulberry, *Morus alba* L. (Wardrop and Waidyarachchi, 2010).

In recent years substantial efforts to discover effective inhibitors of α-glucosidases from natural sources have been made (Benalla et al., 2010; Sim et al., 2010; Miller et al., 2012; Mata et al., 2013). In turn, these inhibitors would be useful for the develop-

☆ Taken in part from the Ph.D. thesis of J. Rivera-Chávez.

* Corresponding author. Tel.: +52 5 55 622 5289; fax: +52 5 55 622 5329.
E-mail address: rachel@unam.mx (R. Mata).

0031-9422/$ - see front matter © 2013 Elsevier Ltd. All rights reserved.
http://dx.doi.org/10.1016/j.phytochem.2013.05.021

ment of new drugs for the treatment of diabetes. In this scenario, the present investigation was undertaken to find new inhibitors of α-glycosidases from a new fungal species belonging to the *Chaetomiaceae* family (MEXU 27095) using *in vitro*, *in silico* and *in vivo* studies. MEXU 27095 is an endophyte associated with *Hintonia latiflora* (Sesse & Moc. ex DC.) Bullock (Rubiaceae), a medicinal antidiabetic plant which possesses 4-phenylcoumarins and cucurbitacins with hypoglycemic and antihyperglycemic properties (Guerrero-Analco et al., 2007; Mata et al., 2013).

2. Results and discussion

2.1. Isolation of α-glucosidase inhibitors

As a part of our program to discover new inhibitors of α-glucosidases from natural sources, a few endophytic fungi associated with *H. latiflora* were isolated and cultured. Organic soluble extracts were prepared and tested *in vitro* against α-glucosidase from *Saccharomyces cerevisiae* (*αGHY*) using a well-known spectrophotometric procedure (Oki et al., 1999). An extract of MEXU 27095 was selected for chemical analysis based on its potent inhibitory activity against *αGHY* (IC_{50} = 46.4 μg/ml). Bioassay-guided fractionation of this extract using different chromatographic procedures led to isolation of tridepsides **1**–**3**, which were characterized as thielavins A (**1**), J (**2**) and K (**3**) by comparison of their spectroscopic and spectrometric data with those previously described (Kitahara et al., 1981; Sakemi et al., 2002). The spectroscopic data are provided in the Supplementary material (Table S1 and Figs. S1–S6).

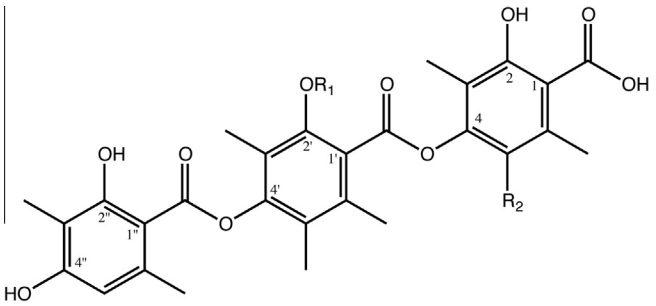

	R_1	R_2
1	H	Me
2	Me	H
3	Me	Me

2.2. α-Glucosidases inhibition evaluation and kinetic studies

Thielavins **1**–**3** inhibited *aGHY* in a concentration-dependent manner with IC_{50} values of 23.8, 15.8 and 22.1 μM, respectively, establishing that the small differences in the structures have little impact on enzymatic inhibitory activity. The three tridepsides were more potent than acarbose (positive control, IC_{50} = 545.4 μM) against *aGHY*, a type I α-glucosidase which hydrolyzes heterogeneous substrates including sucrose and *p*NPG. On the other hand, acarbose was a better inhibitor (IC_{50} of 0.015 μM) of α-glucosidase from *Bacillus stearothermophilus* (*αGHBs*) than thielavin J (**2**), which exhibited an IC_{50} of 30.5 μM; *αGHBs* is a type IV α-glucosidase with maltase activity. These differences in activity against α-glucosidases from different sources are well documented and explained in terms of enzyme substrate recognition (Oki et al., 1999; Nakai et al., 2005). The corresponding graphics for the calculation of the IC_{50} values are included in the supplementary information (Figs. S7 and S8).

In order to obtain further evidence of the nature of the interaction of **1**–**3** with *αGHY* kinetic analyses were carried out. Acarbose was also included in the study. Lineweaver–Burk plots were constructed using different concentrations of inhibitors. The results in Fig. 1 indicated that **1**–**3** showed typical reversible-non-competitive plots, with series of lines with different slopes intersecting in the second quadrant between *x*–*y* axes. The calculated k_i and α values were 27.8, 66.2 and 55.4 μM, respectively (α = 1.0, 1.2, 0.7, respectively). These results suggested that **1**–**3** bind to *αGHY* or to the substrate-enzyme complex (*p*NPG-*αGHY* in this case) (Segel, 1993; Copeland, 2000; Xu, 2010). Acarbose (k_i = 156.1 μM), on the other hand, behaved as competitive inhibitor.

Lineweaver–Burk plots (Fig. 2) generated for the interaction of *αGHBs* with **2** (k_i = 20.0 μM) and acarbose (k_i = 0.008 μM) established that both substances acted as non-competitive inhibitors against this enzyme. Altogether, these results indicated that compound **1–3** could better inhibit *in vivo* the activity of sucrase type of α-glucosidases.

2.3. Molecular modeling and docking studies

In order to envisage the mode of interaction of compound **1**–**3** with *αGHY* and *αGHBs* docking analyses were carried out (Morris et al., 1998; Rudnitskaya et al., 2010). Molecular dockings were performed using a homologated structure for *αGHBs* (maltase), and a crystallized glucose-α-glucosidase (isomaltase–sucrase) complex for *αGHY*. The latter structure (PDB: 3A4A) was obtained from the Protein Data Bank (http://www.rcsb.org/). Before molecular docking of thielavins **1**–**3** and acarbose was carried out, a molecular modeling protocol was established and validated for both enzymes with its natural ligands (maltose and isomaltose from crystal structures PDB: 1URG and 3AXH, respectively). The results of the validation indicated that isomaltose did not bind to the catalytic domain of *αGHBs*, confirming that this α-D-glucohydrolase is specific for non-reducing terminal α-1,4 bonds of maltosaccharides (Suzuki et al., 1984; Takii et al., 1996; Tsujimoto et al., 2007). On the other hand, the results obtained for *αGHY* (PDB: 3A4A) showed that isomaltose bound at the catalytic domain but maltose did not (Yamamoto et al., 2004). The validation data are also included in the Supplementary material (Figs. 9–11).

Thielavins **1**–**3** and acarbose were next docked into both α-glucosidase models. The lowest energy conformation obtained for each ligand in a blind docking was selected and re-docked in the binding site in order to get the better model of interaction. In the case of *αGHBs*, the docking results predicted that **1**–**3** bound in the catalytic domain adopting the same conformation. The pocket was found to be composed by Tyr-63, Arg-197, Asp-199, Phe-282, Leu-285, Gly-283, Arg-300, and the main interactions were hydrophobic although hydrogen bonds were observed between Asp-199 (residue involved in the catalytic domain) and the hydroxyl group at C-4″, and between Leu-285 and Arg-300 with the carboxylic residue of compounds **1–3**. The calculated k_i values for **1–3** were 3.0, 4.3 and 3.4 μM, respectively. Fig. 3 shows the results for compound **3**; for compounds **1** and **2** the corresponding drawings are included in the Supplementary material (Figs. 12 and 13, respectively). Acarbose attached to *αGHBs* (Fig. 3) at the catalytic pocket (as maltose and **1–3**) with an estimated k_i of 28 nM, correlating well with the experimental data.

The docking results of tridepsides **1**–**3** and acarbose with *αGHY* showed that the four ligands lodged in the same pocket near the active site. Hydrogen bonds and hydrophobic-contacts were again the most important type of interactions with the enzyme. In all cases, the pocket included Lys-156, Ser-157, Tyr-158, Ser-240, Ser-241, Asp-242, His-280, Ser-304, Asp-307, Pro-312, Leu-213

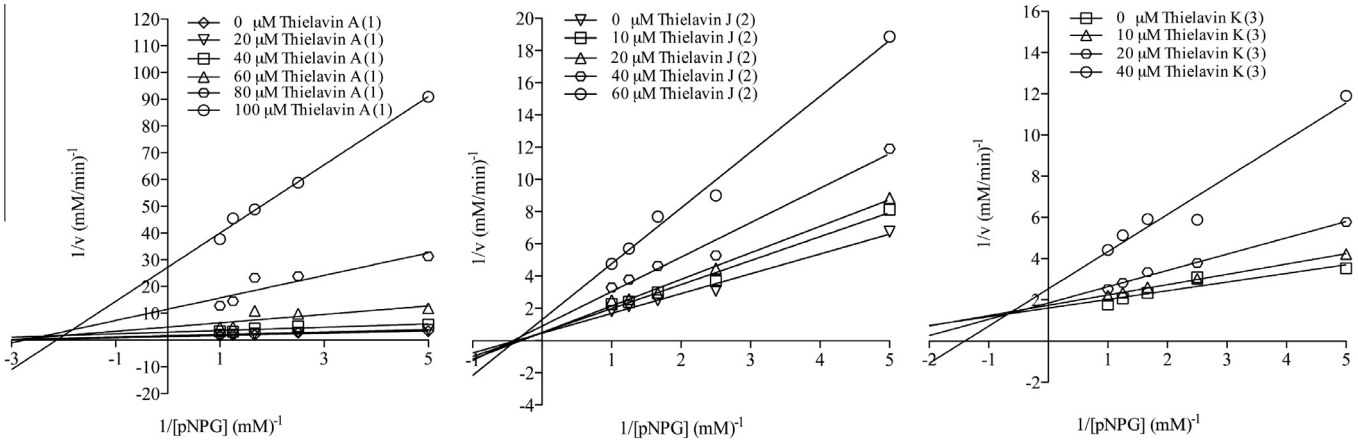

Fig. 1. Lineweaver–Burk plots of *αGHY* inhibition at different concentrations of substrate and thielavins A, J, and K (**1**–**3**).

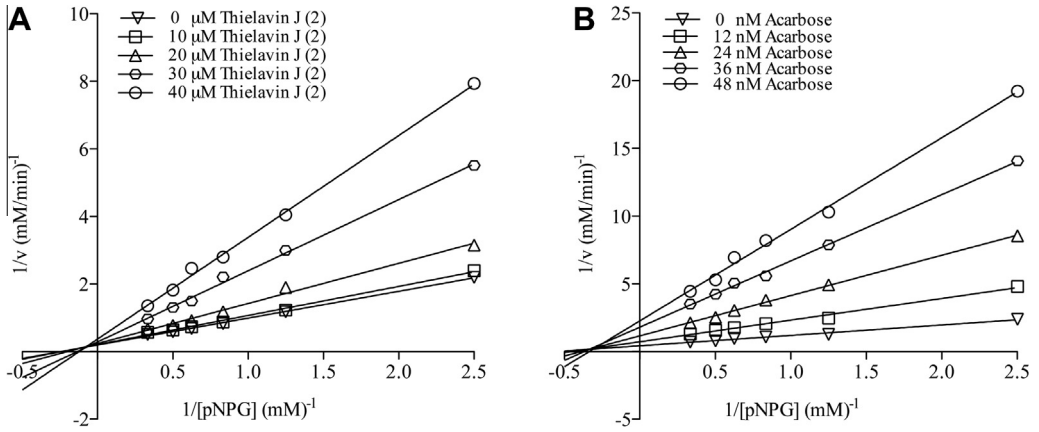

Fig. 2. Lineweaver–Burk plots of *αGHBs* inhibition at different concentrations of substrate and (A) thielavin J (**2**) and (B) acarbose.

and Arg-315. Hydrogen bonds were observed between Ser-240, Ser-241 and Asp-242 and the carboxylic acid residue of **1**–**3**; in addition, the carbonyl ester of the middle C_6–C_1 unit in compounds **1** and **3** displayed hydrogen bond with Arg-315. The theoretical k_i values for **1**–**3** were 11.4, 1.1 and 4.9 μM, respectively. Fig. 4 summarizes the information for compound **3**, and Figs. S14 and S15 illustrated the results for **1** and **2**, respectively.

The theoretical and experimental studies indicated that thielavins **1**–**3** interacted with *αGHBs* and *αGHY* in the same pocket as acarbose adopting a similar conformation as the pseudotetrasaccharide. Furthermore, the *in silico* results supported the outcomes from the experimental kinetic analysis.

2.4. In vivo assays for anti-hyperglycemic and hypoglycemic effect

Thielavin K (**3**), the major tridepside produced by the fungus, was next evaluated to assess its potential antihyperglycemic action using an oral sucrose tolerance test (OSTT) *in vivo*. The OSTT is usually performed to evaluate intestinal α-glucosidase inhibition *in vivo*. Two sets of animals, healthy and diabetic mice were used. Experimental type-II DM was achieved by treating mice with streptozotocin (STZ, 120 mg/kg) 15 min after an injection of nicotinamide (NA, 50 mg/kg). This preliminary treatment with NA provokes partial protection against the cytotoxic action of STZ by scavenging free radicals and causes only minor damage to pancreatic *β*-cell mass creating a diabetic syndrome close to type-II DM (Masiello et al., 1998). This model has recently proven to be a valuable tool for investigation of new antidiabetic agents. Compound **3** was evaluated at a dose range from 3.1 to 31.6 mg/kg. The results of these experiments indicated that **3** decreased glucose blood levels (postprandial peak; $p \leqslant 0.05$) 30 min after oral administration of the sucrose load (3.0 g/kg) in normal mice (Fig. S16) at all doses tested. In NA-STZ diabetic mice only the highest dose (31.6 mg/kg) provoked a significant decrease of blood glucose levels (Fig. 5). The inhibition of postprandial peak was comparable to that of acarbose, used as positive control.

Thielavin K (**3**) was also tested in an acute hypoglycemic experiment *in vivo*. The results indicated that thielavin K (**3**) at the doses of 3.1 and 10 mg/kg decreased blood glucose levels in normal and diabetic mice (Figs. S17 and 6, respectively). In both cases the effect was attained after 5 h and maintained throughout the experiment. Glibenclamide (GLI) was used as positive control in this test.

The results *in vivo* suggest that compound **3** shows potential as antidiabetic agent acting at different targets, namely inhibiting the α-glucosidases at the intestinal levels and other mechanisms yet to be established. In this regard, Sakemi and coworkers (2002) previously demonstrated that **3** inhibited *in vitro* glucose-6-phosphatase (G6Pase); thus, the hypoglycemic effect *in vivo* demonstrated in our study might be also related with the inhibition of G6Pase, which in turn would provoke an important decrease of hepatic glucose output from glyconeogenesis and glycogenolysis.

3. Concluding remarks

Endophytic fungus MEXU 27095 associated with *H. latiflora* biosynthesizes tridepsides **1**–**3** of the thielavins family. These com-

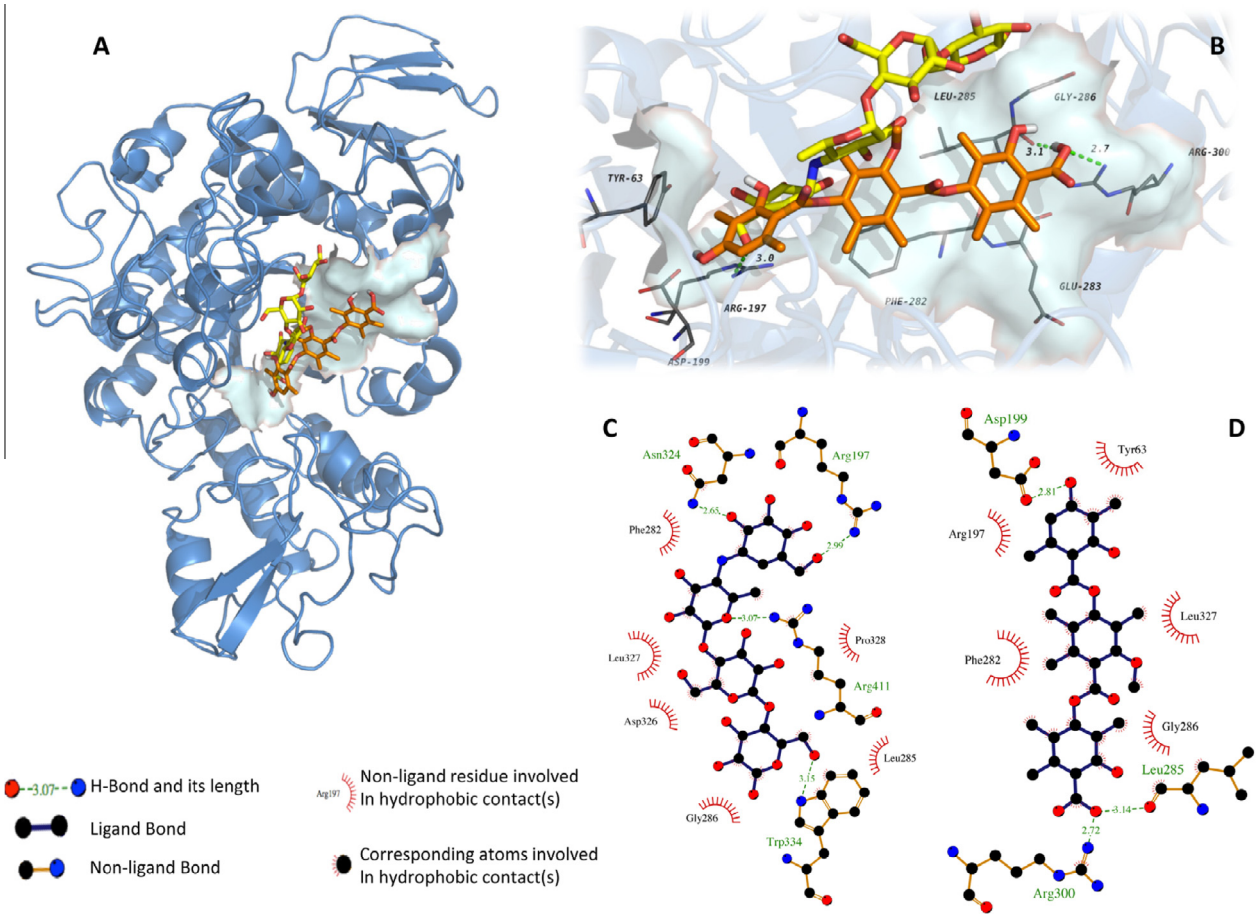

Fig. 3. (A) Structural model of the complex thielavin K (**3**) (orange sticks)-*αGHBs* and acarbose (yellow sticks)-*αGHBs*. (B) 3D Representation of the interaction between thielavin K (**3**), acarbose and *αGHBs* in the binding site predicted. (C) 2D Representation of the interactions among *αGHBs* and acarbose. (D) 2D Representation of the interactions among *αGHBs* and thielavin K (**3**). Graphics generated with PyMol and LigPlot. (For interpretation of the references to colour in this figure legend, the reader is referred to the web version of this article.)

pounds showed a high potential as inhibitors of *αGHY*. Molecular docking of thielavins **1**–**3** with *αGHY* predicted that these compounds adopt a similar conformation and bind in a similar site as acarbose. *In vivo* evaluation of **3** showed that this compound decreased fasting and postprandial glucose levels in a TII-DM animal model. Thus thielavin-type tridepsides represent a new class of α-glucosidase inhibitors. Likewise our results confirmed that endophytic fungi from medicinal plants are good sources for the discovery of new leads for drug development.

4. Experimental

4.1. Reagents

p-Nitrophenyl-α-D-glucopyranoside (*p*NPG), streptozotocin 98%, nicotinamide, glibenclamide, sucrose, acarbose, and α-glucosidases from *Bacillus stearothermophilus* and *Saccharomyces cerevisiae* were purchased from Sigma–Aldrich St. Louis, MO, USA. All other chemicals used in this study were of analytical grade.

4.2. General experimental procedures

IR spectra were obtained using a Perkin-Elmer Spectrophotometer 400 FT-IR. NMR spectra including HSQC, and HMBC were recorded in MeOH-d_4 or in a mixture of $CDCl_3$–MeOH-d_4 (7:3) using a Varian Inova 500 spectrometer at 500 (^{1}H) and 125 MHz (^{13}C), with tetramethylsilane (TMSi) as an internal standard; chemical shifts were recorded as δ values. Electrospray ionization mass spectra were recorded on a Thermo Scientific LTQ Orbitrap XL hybrid FTMS (Fourier Transform Mass Spectrometer) in the positive or negative ionization mode. HPLC separations were performed using a Symmetry RP column [7.8 × 300 mm, and 3.0 ml/min] and CH_3CN (acidified with HCO_2H at 0.5%). Control of the equipment, data acquisition, processing, and management of chromatographic output was performed by the Empower® 2 software program (Waters). The absorbance in the enzymatic assay was determined at 405 nm in a BIO-RAD microplate reader model 680. Column chromatography (CC) was carried out on either Sephadex® LH-20 (Sigma–Aldrich–Fluka) or silica gel 60 (70–230 mesh, Merck). Thin layer chromatography (TLC) analyses were carried out on silica gel 60 F_{254} plates (Merck) using ceric sulphate (10%) solution in H_2SO_4 as color reagent.

4.3. Plant material

H. latiflora leaves were collected and identified by Sol Cristians-Niizawa in Huetamo (18°31.709′N, 101°4.692′W; 221 masl), State of Michoacán, México, in July 2010. A voucher specimen (131,316) was deposited at the Herbarium of the School of Sciences (FCME), Universidad Nacional Autónoma de México, Mexico City.

4.4. Fungus isolation and identification

The endophytic fungus MEXU 27905 was isolated from selected healthy leaves of *H. latiflora*. A strong surface sterilization protocol was applied to 1 g of leaves (Rodriguez et al., 2009). Complete in-

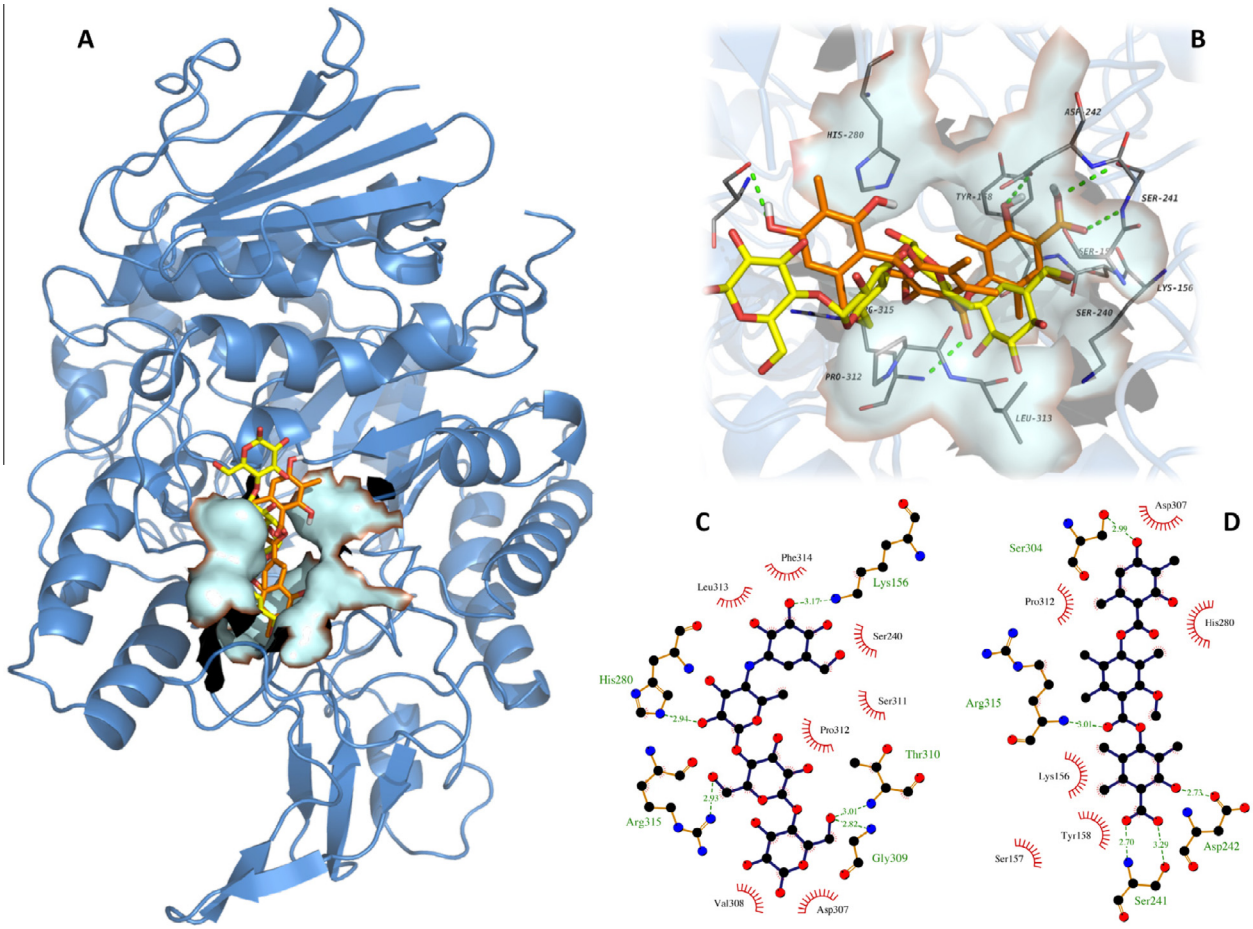

Fig. 4. (A) Structural model of the complex thielavin K (**3**) (orange sticks)-*αGHY* and acarbose (yellow sticks)-*αGHY*. (B) 3D Representation of the interaction between thielavin K (**3**), acarbose and *αGHY* in the binding site predicted. (C) 2D Representation of the interactions between *αGHY* and acarbose (2D). (D) 2D Representation of the interactions between *αGHY* and thielavin K (**3**). Graphics generated with PyMol and LigPlot. (For interpretation of the references to colour in this figure legend, the reader is referred to the web version of this article.)

tact leaves were immersed in EtOH–H_2O (50 ml, 75:25, v/v) (1 min), 3.4% aqueous NaOCl solution (10 min) and EtOH–H_2O (50 ml, 75:25, v/v) (1 min); afterward the sterilized leaves were rinsed with sterile distilled H_2O and dried with sterile absorbent paper. Sterilized leaves were cut into 5 × 5 mm pieces and deposited on a Petri dish (3–5 pieces by plate) containing PDA (potato-dextrose agar; Difco) and streptomycin sulfate (4 μg/ml) and cyclosporine A (5 μg/ml). The pure fungal strain was obtained after serial transfers on PDA and was deposited in the fungal collections of the Herbario Nacional de Mexico (MEXU) under the accession number of MEXU 27095. Sequence data (28S ribosomal RNA and internal transcribed spacer (ITS) region) were deposited in GenBank as accessions JX292135 and JX292136, respectively. Data available at GenBank aligning with MEXU 27905 suggested this fungus is a member of the Chaetomiaceae (Fig. S18).

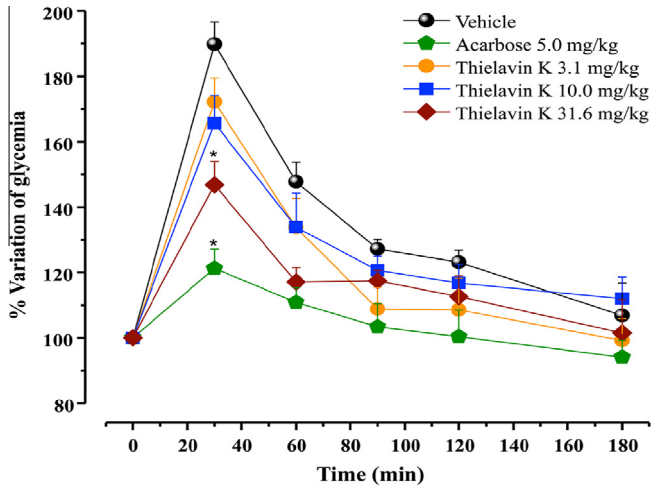

Fig. 5. Influence of thielavin K (**3**) on blood glucose levels in NA-STZ-diabetic mice during an OSTT. *$p < 0.05$ significantly different ANOVA followed by Dunnett's t test.

4.5. Fermentation, extraction and isolation

MEXU 27095 was cultured in 15 Petri dishes containing 120 ml of solid media PDA. After 20 days of fungal growth at 25 °C, the culture media was extracted exhaustively with CH_2Cl_2–MeOH 9:1 (3 × 2 L) and the resulting extract was evaporated *in vacuo* to yield a brown solid residue (4.1 g). The crude extract was fractionated by open silica-gel cc, eluting with a gradient of hexane-CH_2Cl_2 (10:0 → 0:10) and CH_2Cl_2–MeOH (10:0 → 5:5), respectively. Each fraction was monitored by TLC, and fractions with similar patterns were combined to yield six primary fractions (F_I–F_{VI}). F_{VI} (500 mg), the most active fraction (98.9% of inhibition) in a preliminary α-glucosidase inhibition test using *αGHY* (Oki et al., 1999), was subjected to open Sephadex® LH-20 cc eluting with MeOH to yield four secondary fractions (F_{VI-1}–F_{VI-4}). The resolution of fraction F_{VI-4} (390 mg) by reversed phase HPLC led to the isolation of thielavin A (**1**, 31.3 mg), thielavin J (**2**, 60.2 mg) and thielavin K (**3**,

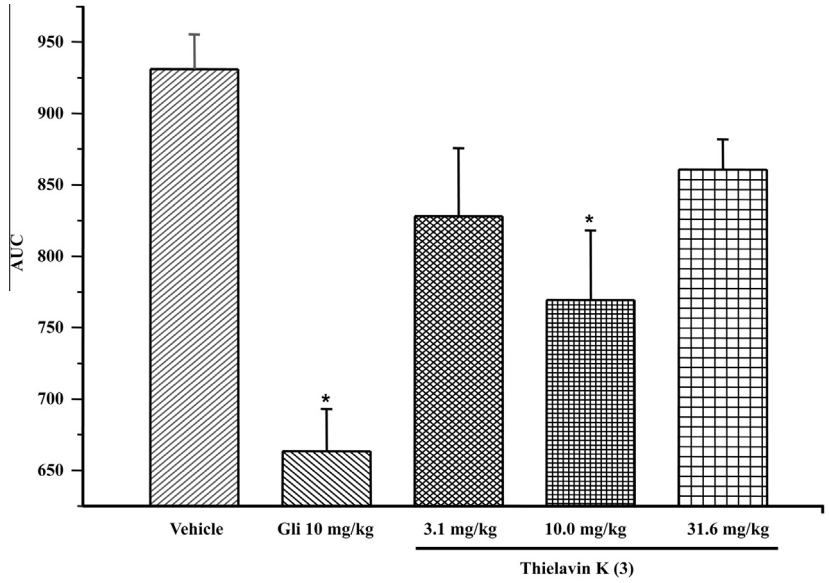

Fig. 6. Influence of thielavin K (**3**) on blood glucose levels in NA-STZ-diabetic mice using the acute hypoglycemic test. Each value is the mean ± SEM for six mice in each group. $^{*}p < 0.05$ significantly different ANOVA followed by Dunnett's *t*-test.

68.5 mg) as glassy solids. Their IR, NMR and MS were identical to those previously reported (Kitahara et al., 1981; Sakemi et al., 2002).

4.6. Assay for α-glucosidase inhibitors

The fungal extract, fractions, compounds **1**–**3** and acarbose (positive control) were dissolved in either MeOH or phosphate buffer solution (PBS, 100 mM, pH 7). Aliquots of 0–10 μl of testing materials (triplicated) were incubated for 10 min with 20 μl of enzyme stock solution (0.4 units/ml of *αGHBs* or 0.75 units/ml of *αGHY* in PBS). After incubation, 10 μl of substrate [*p*NPG, 10 mM for *αGHBs* and 5 mM for *αGHY*] was added and incubated for 20 min at 37 °C. Absorbance at 405 nm was then determined (Oki et al., 1999).

The inhibitory activity of the fungal extract and fractions was determined as a percentage in comparison to a blank according with the following equation:

$$\%\alpha GHY = \left(1 - \frac{A_{405}t}{A_{405}c}\right) \times 100\%$$

where $\%\alpha GHY$ is the percentage of inhibition, $A_{405}t$ is the corrected absorbance of extract, fraction or compound under testing $(A_{405end} - A_{405initial})$ and $A_{405}c$ is the absorbance of blank $(A_{405endblank} - A_{405initialblank})$. The concentration required to inhibit activity of the enzyme by 50% (IC_{50}) was calculated by regression analysis (Figs. S7 and S8), using the following equation:

$$\%Inhibition = \frac{A_{100}}{1 + \left(\frac{I}{IC_{50}}\right)^{S}}$$

where A_{100} is the maximum inhibition, I is the inhibitor concentration, IC_{50} is the concentration required to inhibit activity of the enzyme by 50%, and *s* is the cooperative degree (Copeland, 2000).

The mode of inhibition of α-glucosidase was determined by the Lineweaver–Burk plots. Dixon plots were used to determine the inhibitory constants. The inhibition is described by the following equation:

$$V = \frac{V_{max}S}{k_m\left(1 + \frac{[I]}{k_i}\right) + s\left(1 + \frac{[I]}{\alpha k_i}\right)}$$

where *v* is the initial velocity in the absence and presence of the inhibitor, *S* and *I* respectively are the concentration of substrate and inhibitor, V_{max} is the maximum velocity, k_m is the Michaelis–Menten constant, k_i is the competitive inhibition constant, and αk_i is the uncompetitive inhibition constant. The kinetic data were analyzed using Origin 8.0 software.

4.7. Computational methods

4.7.1. Proteins

A three dimensional model of *αGHBs* was built by comparative modeling using the SWIS-MODEL program (automated protein structure homology-modeling server; http://swissmodel.expasy.org). The crystallographic structure of the related GH-13 α-glycosidase from *Geobacillus* sp. strain HTA-462 (PDB: 2ZE0; Shirai et al., 2008) was selected as template due to its highest sequence identity (94%) with respect to *αGHBs*. The homology modeling begins with the retrieval of the amino acid sequence of *B. stearothermophilus* exo-α-glycosidase (EC 3.2.1.20) which comprises 555 amino acid residues (GenBank accession: D84648.1; NCBI http://www.ncbi.nlm.nih.gov). The modeled protein was optimized geometrically with the program HyperChem 8 and validated using the ProCheck (stereochemical quality analysis software) program (Laskowski et al., 1993, 1996). Yeast isomaltase (*αGHY*) crystallographic structure was downloaded from the Protein Data Bank site (PDB: 3A4A). Subsequently all hydrogen and Kolleman charges were assigned to both receptors using AutoDockTools 1.5.4. The files were saved in proper format for use with Autogrid4.0 and AutoDock4.0 systems.

4.7.2. Ligands

Compounds **1**–**3** were built using the program Spartan'02 (www.wavefunction.com) and optimized geometrically using the program Gaussian 09, revision A.02 (Gaussian Inc., Wallingford, CT, USA) at DFT B3LYP/DGDZVP level of theory. The ligands were prepared by assigning the Gasteiger-Marsilli atomic charges and nonpolar hydrogens using AutoDockTools 1.5.4 (http://mgltools.scripps.edu/).

4.7.3. Docking

Binding pockets of enzymes and docking simulation were predicted using AutoDock 4.0 (http://autodock.scripps.edu/; (Morris et al., 1998; Rudnitskaya et al., 2010; Çifci et al., 2012). Initially, a blind docking was performed at the interface as the first ligand binding position; then, the best energy result of the previous procedure was used as initial conformation to undertake simulation. Docking studies were done with Lamarckian Genetic Algorithm (LGA). Grid box for docking was set around central atom of the ligand with dimension of $40 \times 40 \times 40$ Å. Parameters were set to a LGA calculation of 250 runs, whereas energy evaluations were set to 2,500,000 and 27,000 generations (repetition of process). The obtained docked poses were analyzed with AutoDockTools using cluster analysis, PyMOL (De Lano and Scientific, 2002) and LIGPLOT$^+$ (www.ebi.ac.uk).

4.8. In vivo assays for anti-hyperglycemic and hypoglycemic actions

4.8.1. Experimental animals

All animal assays were conducted both in normoglycemic and diabetic mice (Verspohl, 2002; Escandón-Rivera et al., 2012). Male ICR mice, weighing 20–25 g and 20–25 days old, were obtained from Centro UNAM Harlan (Harlan México, SA de CV). All procedures involving animals were conducted in agreement with the Mexican Official Norm for Animal Care and Handling (NOM-062-ZOO-1999) and in compliance with international rules on care and use of laboratory animals. The animals were contained in groups of eight under standard laboratory conditions (12 h light–dark cycle under controlled temperature, 22 ± 1 °C) and maintained on a standard pellet diet and water *ad libitum*.

4.8.2. Preparation of the test samples

Thielavin K (**3**) was suspended in saline solution. Glibenclamide (10 mg/kg) was used as hypoglycemic control drug. Acarbose (5 mg/kg) was used as an anti-hyperglycemic drug. Sucrose (3 g/kg) was used for the carbohydrate tolerance test. Control mice group received only saline solution. All animals were orally administered (Escandón-Rivera et al., 2012).

4.8.3. Induction of type II DM (experimental model)

Type II DM was induced by i.p. admisnistration of freshly prepared STZ (120 mg/kg) dissolved in 0.M citrate buffer, pH 4.5, 15 min after an injection of NA (50mg/kg) dissolved in distilled water as previously described (Escandón-Rivera et al., 2012).

4.8.4. Collection of blood samples and determination of blood glucose levels

Blood samples were collected from the caudal vein by means a small incision at the end of the tail. Blood glucose levels (mg/dl) were estimated by the enzymatic glucose oxidase method using a commercial glucometer (One Touch Ultra 2, Johnson & Johnson, CA, USA). The percentage variation of glycaemia for each group was calculated with respect to the initial (0 h) level, according to the following equation, where G_i is initial glycaemia value and G_t is the glycaemia value after treatment administration (Verspohl, 2002):

$$\%Variation\ of\ glycemya = \left(\frac{G_t}{G_i}\right)100$$

4.8.5. Acute hypoglycemic assay

Normal and diabetic animals were placed in acrylic boxes in groups of six deprived of food but free access to water 4 h before experimentation. Thielavin K (**3**) was orally administered (3.1, 10.0 y 31.6 mg/kg of body wt) to three different groups of animals; GLI (10 mg/kg) and saline solution were given as positive control and vehicle, respectively to two other groups of animals. Glibenclamide and **3** were suspended in the vehicle. Blood samples were collected at 0, 1.5, 3, 5, 7 and 9 h after administrations (Escandón-Rivera et al., 2012). Area under the curve (AUC) was calculated applying the following equation:

$$AUC = \Sigma\left(\frac{\%VG_{T1} + \%VG_{T2}}{2}\right)(T_2 - T_1)$$

where $\%VG_{T1}$ and $\%VG_{T2}$ represent the percentage variation of glycaemia at 0, 1.5, 3, 5, 7 and 9 h after oral sucrose feeding to mice.

4.8.6. Oral sucrose tolerance test

Both groups of mice (normal and diabetic) were placed in acrylic boxes forming groups of six animals (I–V). Group I was administrated with the vehicle; group II received acarbose; group III to V received different amounts of thielavin K (**3**) (3.1, 10.0 and 31.6 mg/kg of body wt). Time 0 min was measured before treatment with compound **3** or control; 30 min later a sucrose load (3.0 g/kg) was given to the animals. Blood samples were obtained 30, 60, 90, 120, and 180 min after the carbohydrate load.

4.8.7. Statistical analysis

Results are expressed as the mean ± SEM of six animals in each group. Analysis of variance (ANOVA, one way) was used to analyze changes in the percentage variation of glycaemia followed by Dunnett's test; $p < 0.05$ was considered statistically significant. Sigma stat software was used for data analysis.

Acknowledgments

This work was supported by a grant from CONACyT (99395). We thank G. Duarte, M. Guzmán, M. Gutierrez, I. Rivero, A. Pérez, G. Anaya and S. Cristians for their valuable technical assistance. J. Rivera-Chávez acknowledges a fellowship from CONACyT to pursue graduate studies.

Appendix A. Supplementary data

Supplementary data associated with this article can be found, in the online version, at http://dx.doi.org/10.1016/j.phytochem.2013.05.021.

References

Benalla, W., Bellahcen, S., Bnouham, M., 2010. Antidiabetic medicinal plants as a source of alpha glucosidase inhibitors. Curr. Diabetes Rev. 6, 247–254.
Chen, L., Magliano, D.J., Zimmet, P.Z., 2011. The worldwide epidemiology of type 2 diabetes mellitus-present and future perspectives. Nature Publishing Group 8, 228–236.
Copeland, R.A., 2000. Enzymes: A Practical Introduction to Structure, Mechanism, and Data Analysis, second ed. Wiley-VCH.
Çifci, G., Aviyente, V., Akten, E.D., 2012. Molecular Docking study based on pharmacophore modeling for novel phosphodiesterase IV inhibitors. Mol. Inf. 31, 459–471.
De Lano, W., Scientific, L.D., 2002. De Lano: PyMOL version 0.99, DeLano Scientific.
Escandón-Rivera, S., González-Andrade, M., Bye, R., Linares, E., Navarrete, A., Mata, R., 2012. α-Glucosidase inhibitors from *Brickellia cavanillesii*. J. Nat. Prod. 75, 968–974.
Guerrero-Analco, J., Medina-Campos, O., Brindis, F., Bye, R., Pedraza-Chaverri, J., Navarrete, A., Mata, R., 2007. Antidiabetic properties of selected Mexican copalchis of the Rubiaceae family. Phytochemistry 68, 2087–2095.
Israili, Z.H., 2011. Advances in the treatment of type 2 diabetes mellitus. Am. J .Ther. 18, 117–152.
Kitahara, N.N., Endo, A.A., Furuya, K.K., Takahashi, S.S., 1981. Thielavin A and B, new inhibitors of prostaglandin biosynthesis produced by *Thielavia terricola*. J. Antibiot. 34, 1562–1568.
Laskowski, R.A., MacArthur, M.W., Moss, D.S., Thornton, J.M., 1993. PROCHECK: a program to check the stereochemical quality of protein structures. J. Appl. Crystallogr. 26, 283–291.

Laskowski, R.A., Rullmannn, J.A., MacArthur, M.W., Kaptein, R., Thornton, J.M., 1996. AQUA and PROCHECK-NMR: programs for checking the quality of protein structures solved by NMR. J. Biomol. NMR 8, 477–486.

Mata, R., Cristians, S., Escandón-Rivera, S., Juárez-Reyes, K., Rivero-Cruz, I., 2013. Mexican antidiabetic herbs: valuable sources of inhibitors of α-glucosidases. J. Nat. Prod. 130304132955004.

Miller, K.I., Qing, C., Sze, D.M.-Y., Roufogalis, B.D., Neilan, B.A., 2012. Culturable endophytes of medicinal plants and the genetic basis for their bioactivity. Microb. Ecol. 64, 431–449.

Morris, G.M., Goodsell, D.S., Halliday, R.S., Huey, R., Hart, W.E., Belew, R.K., Olson, A.J., 1998. Automated docking using a Lamarckian genetic algorithm and an empirical binding free energy function. J. Comput. Chem. 19, 1639–1662.

Nakai, H., Okuyama, M., Kim, Y., Saburi, W., Wongchawalit, J., Mori, H., Chiba, S., Kimura, A., 2005. Molecular analysis of a-glucosidase belonging to GH-family 31. Biologia, Bratislava 60, 131–135.

Oki, T., Matsui, T., Osajima, Y., 1999. Inhibitory effect of α-glucosidase, inhibitors varies according to its origin. J. Agric. Food Chem. 47, 550–553.

Rodriguez, R.J., White Jr., J.F., Arnold, A.E., Redman, R.S., 2009. Fungal endophytes: diversity and functional roles. New Phytol. 182, 314–330.

Rudnitskaya, A., Török, B., Török, M., 2010. Molecular docking of enzyme inhibitors. Biochem. Mol. Biol. Educ. 38, 261–265.

Sakemi, S.S., Hirai, H.H., Ichiba, T.T., Inagaki, T.T., Kato, Y.Y., Kojima, N.N., Nishida, H.H., Parker, J.C.J., Saito, T.T., Tonai-Kachi, H.H., VanVolkenburg, M.A.M., Yoshikawa, N.N., Kojima, Y.Y., 2002. Thielavins as glucose-6-phosphatase (G6Pase) inhibitors: producing strain, fermentation, isolation, structural elucidation and biological activities. J. Antibiot. 55, 941–951.

Scully, T., 2012. Diabetes in numbers. Nature 485, S2–S3.

Segel, I.H., 1993. Enzyme Kinetics. Wiley-Interscience.

Shirai, T., Hung, V.S., Morinaka, K., Kobayashi, T., Ito, S., 2008. Crystal structure of GH13 α-glucosidase GSJ from one of the deepest sea bacteria. Proteins 73, 126–133.

Sim, L., Jayakanthan, K., Mohan, S., Nasi, R., Johnston, B.D., Pinto, B.M., Rose, D.R., 2010. New glucosidase inhibitors from an Ayurvedic herbal treatment for type 2 diabetes: structures and inhibition of human intestinal maltase-glucoamylase with compounds from salacia reticulata. Biochemistry 49, 443–451.

Suzuki, Y., Shinji, M., Eto, N., 1984. Assignment of a *p*-nitrophenyl α-D-glucopyranosidase of *Bacillus stearothermophilus* ATCC 12016 to a novel exo-α-1,4-glucosidase active for oligomaltosaccharides and α-glucans. Biochim. Biophys. Acta (BBA) – Protein Struct. Mol. Enzymol. 787, 281–289.

Takii, Y., Takahashi, K., Yamamoto, K., Sogabe, Y., Suzuki, Y., 1996. *Bacillus stearothermophilus* ATCC12016 α-glucosidase specific for α-1,4 bonds of maltosaccharides and α-glucans shows high amino acid sequence similarities to seven α-D-glucohydrolases with different substrate specificity. Appl. Microbiol. Biotechnol. 44, 629–634.

Tsujimoto, Y., Tanaka, H., Takemura, R., Yokogawa, T., Shimonaka, A., Matsui, H., Kashiwabara, S.I., Watanabe, K., Suzuki, Y., 2007. Molecular determinants of substrate recognition in thermostable α-glucosidases belonging to glycoside hydrolase family 13. J. Biochem. 142, 87–93.

Verspohl, E.J., 2002. Recommended testing in diabetes research. Planta Med. 68, 581–590.

Wardrop, D.J., Waidyarachchi, S.L., 2010. Synthesis and biological activity of naturally occurring α-glucosidase inhibitors. Nat. Prod. Rep. 27, 1431.

Xu, H., 2010. Inhibition kinetics of flavonoids on yeast-glucosidase merged with docking simulations. Protein Pept. Lett. 17, 1270–1279.